Al-5 wt% Al_2O_3 Metal Matrix Composite Prepared by Mechanical Alloying: Effect of Milling Time and Sintering Temperature

M.F. Zawrah [1], Mohammed A. Taha [2], F.A. Saadallah [2], A.G. Mostafa [3]*, M.Y. Hassaan [3] and Mahmoud Nasr [2]

[1.] Ceramics Department, National Research Center, Dokki, Cairo, Egypt
[2.] Solid State Physics Department, National Research Center, Dokki, Cairo, Egypt
[3.] Physics Department, Faculty of Science, Al-Azhar University, Nasr City, Cairo, Egypt
*drahmedgamal@yahoo.com

Abstract: Al-5 wt% Al_2O_3 metal matrix composite (MMC) was synthesized by mechanical alloying technique. The effect of milling time (1, 3, 5 and 7 h) and consequently the distribution of Al_2O_3 through the Al matrix, on the properties of the obtained powder composites were studied. X-ray diffraction (XRD) and transmission electron microscopy (TEM) were used to investigate their phase composition and morphology. The powders were cold pressed under 10 MPa and sintered in argon atmosphere at different temperatures (300, 370 and 470 °C) for 1 h. The relative density and apparent porosity of the sintered samples were determined by Archimedes method, their microstructure was investigated by using scanning electron microscopy (SEM) attached with energy dispersive spectrometer unit (EDS) and their micro-hardness was conducted by Vickers indentor. The results showed that no notification of phase changes during milling, and as the milling time was gradually increased the crystallite size decreased, while the internal micro-strain increased. It was found also that the relative density increased with increasing milling time and sintering temperature, while the apparent porosity decreased. The micro-hardness of the sintered composites increased with increasing milling time.

1. Introduction

Recently, metal matrix composites are the subject of extensive research and development activities, because of their interesting specific properties. Most of the recent research concerned with aluminum and other light metal matrices for applications requiring light weight in combination with high strength and stiffness. The conventional aluminum alloys are usually used in numerous applications, where their excellent strength, ductility and corrosion resistant properties are well established and they can be modified to fulfill the requirements of other new applications. Also, aluminum matrix can be reinforced by various types of reinforcements in the form of particles, whiskers or short fibers [1, 2]. Reinforcing the ductile aluminum matrix with stronger and stiffer second-phase (e.g. oxides, carbides, borides, and nitrides) provides combined properties of both the metallic matrix and the ceramic reinforcement components resulting in improved physical and mechanical properties [3]. It was found that, both uniform distribution of the fine reinforcements and the fine grain size of the matrix act also to improve the mechanical properties of the prepared composites. Moreover, the mechanical properties of the resulting composites tend to be improved with increasing volume fraction and decreasing particle size of the reinforcements [4, 5].

Mechanical alloying (MA) is a simple and important technique for attaining a homogeneous distribution of the fine particles within a fine grained matrix [6. 7]. It is a powder processing method in which powder particles can dispraised throughout the metal matrix, during a repeated process of cold welding, fracturing, and re-welding in a high-energy ball mill. The powder particles will be cold welded due to the mechanical forces and the repetition of work stress hardness the particles. Consequently, the powder particles become brittle and fracture. This, in turn, produces fresh surfaces, which facilitates further cold welding [8]. Since MA is a kind of high energy rate milling, thus all the effective milling parameters affect directly the obtained composite and hence an improvement of the mechanical and physical properties of the resulting alloy can be easily achieved [9].

The main goal of the current work is to study the influence of milling time and hence the distribution of reinforcement phase (Al_2O_3) on the properties of Al-5 wt% Al_2O_3 nanocomposite powders fabricated by mechanical alloying. Moreover, the sintering of the obtained powder nano-composites is also followed at different sintering

temperatures. The physical and mechanical properties of the sintered bodies are correlated to the studied parameters.

2. Materials and Experimental Procedures

Highly pure Al (99%) and Al_2O_3 (98.2%) having average particle sizes less than 74 & 1.5 μm respectively, were used as starting raw materials to prepare Al-5 wt% Al_2O_3 metal matrix composite. Stearic acid was used as process controlling agent to prevent agglomeration of the powder mixture during milling.

A planetary ball mill (model: SFM-1 Desk-Top Planetary Ball Mill) using Al_2O_3 - ZrO_2 balls having different diameters (6-20 mm) was used. The rotating speed was 500 rpm and the ball-to-powder weight ratio was 10:1.

Phase identification of the milled powders was conducted by X-ray diffraction (XRD) analysis using "Philips PW 1373" X-ray diffractometer with CuK_{α}-Ni filtered radiation. The lattice parameter "a" of the obtained phases was calculated for the principle planes (111, 200, 220 and 311), from the obtained XRD data according to the following equation [10]:

$$\frac{1}{d^2} = \frac{h^2 + k^2 + l^2}{a^2} \qquad (1)$$

Where d is the inter planes spacing.

XRD data was also used to determine the crystallite size (D) and lattice strain (ε). The crystallite size was determined from the peaks broadening at half maxium (B) of the diffraction lines 111, 200, 220 and 311, using Scherrer equation [11, 12]:

$$D = \frac{0.9\lambda}{B \cos \theta} \qquad (2)$$

Where; λ is the wave length = 1.54059˚A (Cu-Ni radiation), B is the full width at half maximum, θ is the angle in radians.
Lattice strain (ε) could be also calculated for the same diffraction lines applying the following equation [13, 14]:

$$\varepsilon = \frac{B}{4\tan \theta} \qquad (3)$$

Transmission electron microscope (TEM), (model JEOL JEM-1230), operating at 120 kV and attached with a charge coupled device (CCD) camera, was employed to investigate the morphology

and particle size of the milled powders after different milling times.

The powder composites were then compacted at room temperature into samples of 10 mm diameter and 4 mm thickness using a hardened steel pre-compaction die set, and a hydraulic compressor was used for pressing the specimens at 10 MPa. The compacted samples were sintered at three different temperatures (300, 370 and 470°C) in argon atmosphere for one hour and heating rate 8°C/min.

The relative density (RD) and apparent porosity (AP) of the sintered specimens are measured according to Archimedes principle and applying the following equations,

$$RD = \frac{BD}{TD} \, x100 \, (\%) \qquad (4)$$

$$AP = \frac{W_d - W_i}{W_s - W_i} \, x \, 100 \, (\%) \qquad (5)$$

Where BD and TD are the bulk and theoretical densities, and can be calculated from the equations,

$$BD = \frac{W_d}{W_s - W_i} \, x \, \rho \, (g/cm^3) \qquad \text{and}$$

$$TD = (TD_{Al} \times Vol\%Al) + (TD_{Al_2O_3} \times Vol\%Al_2O_3)$$

Where; W_d is the weight of dry sample, W_s is the weight of saturated sample in kerosene, W_i is the weight of immersed samples in kerosene and ρ is the density of kerosene (0.81 g/cm^3).

The theoretical density (TD) of the compacted samples is calculated using the simple mixture rule, considering the values of fully dense Al and Al_2O_3 (2.70 and 3.95 g/cm^3, respectively).

Scanning electron microscope (SEM) as well as energy dispersive spectroscopy (EDX) "Philips XL30" were also used to characterize the microstructure and the formed phases of the sintered samples. The reinforcement behavior of the resulted composites was estimated by micro-hardness measurement (Vickers hardness) using ASTM: B933-09. 1.961N load for 10 sec. applied during measuring hardness. The obtained hardness values of the investigated materials were calculated as the average of 5 readings along the cross sectional surface of the specimens.

3. Results and Discussion
3.1. Effect of milling time on the obtained powder composites
3.1.1. Phase identification

Fig.s (1&2) show the XRD patterns of the as-received pure Al and Al_2O_3 respectively. These

patterns are then compared with the standard patterns (card number 88-0826&85-1326) to check the present phases [15- 16]. For Al powder, all peaks in the pattern could be identified as Al with cubic crystal structure, while the XRD pattern of Al_2O_3 powder indicated that it belongs to corundum (α-Al_2O_3) type with a rhombohedral crystal structure. It can be noted also that the diffraction peaks are intense and sharp due to their higher crystallinity. The crystal sizes of the as-received Al and Al_2O_3 are 60.6 and 32.37nm, respectively, while the lattice strain is equal to 0.1433 and 0.2629 %, respectively.
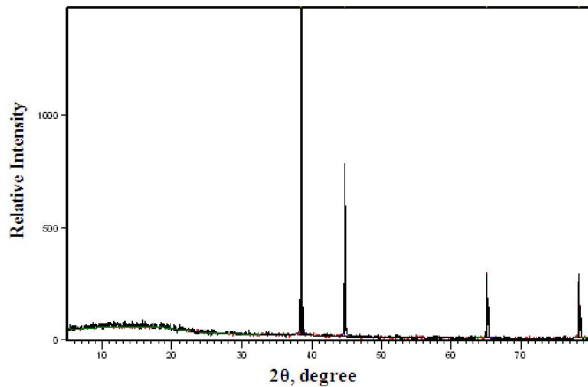

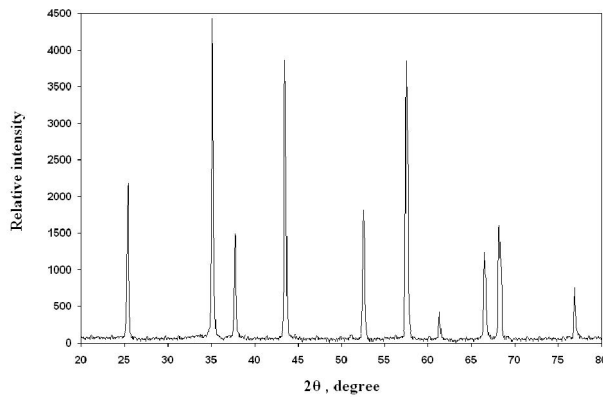Figure 1. XRD pattern of the as-received pure Al.

Figure 2. XRD pattern of the as-received pure Al_2O_3

Fig. (3) shows the XRD patterns of the mechanically alloyed Al- 5wt% Al_2O_3 milled at 1, 3, 5, and 7 h. It is appeared that only two phases of Al and Al_2O_3 are found in the as-milled powders. It is observed also that, with the increase of milling time, the peaks tend to be broadened [17].

The calculated full width at half maximum (FWHM) of the XRD patterns for the milled Al-5 wt% Al_2O_3 powders showed a gradual increase as the milling time was gradually increased, as exhibited in Fig. (4). Such increase may be due to severe lattice distortion and grain size refinement [18].

The relationship between lattice parameters and milling time can be seen in Fig. (5) where, as the milling time was increased the lattice parameters remain constant, which means that neither oxidation of Al nor formation of solid solution between Al and Al_2O_3 has been formed.

The crystallite size and lattice internal micro-strain calculated from the broadening of the XRD peak can be shown in Fig. (6), as a function of milling time. It indicated that, with increasing milling time the crystal size (D) decreased (according to the equation: $D=Kt^{-2}$ where K is a constant), while the lattice micro-strain is found to increase [6, 19]. Similar results were reported for Cu-Al_2O_3 composite [20, 21].

The observed change in both the crystallite size and lattice micro-strain of Al power milled with the hard alumina particles can be attributed to the hindering of the dislocation movement by Orowan bowing mechanism, leading to an increase in the dislocation density, and thereby accelerating the crystal refining progress [22].
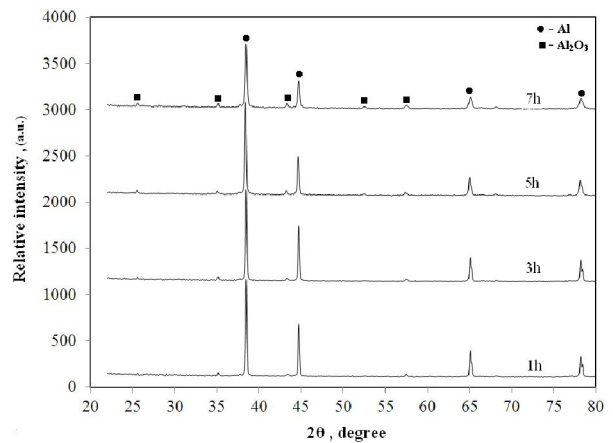

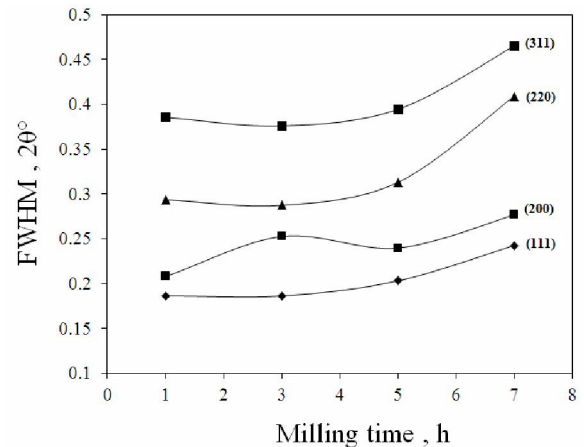Figure 3. XRD patterns of the Al-5 wt% Al_2O_3 powder composites milled for different times

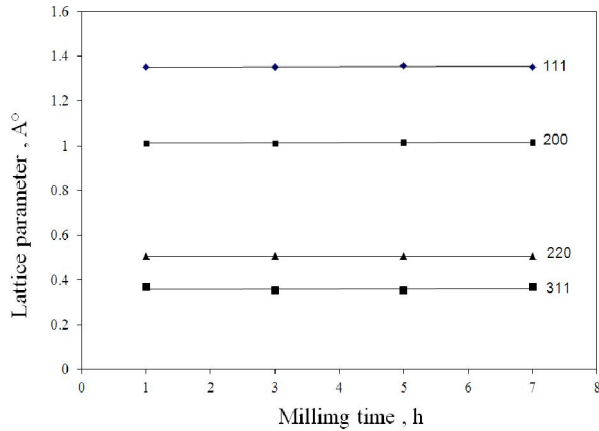Figure 4. FWHM for the milled Al-5 wt% Al_2O_3 versus milling time

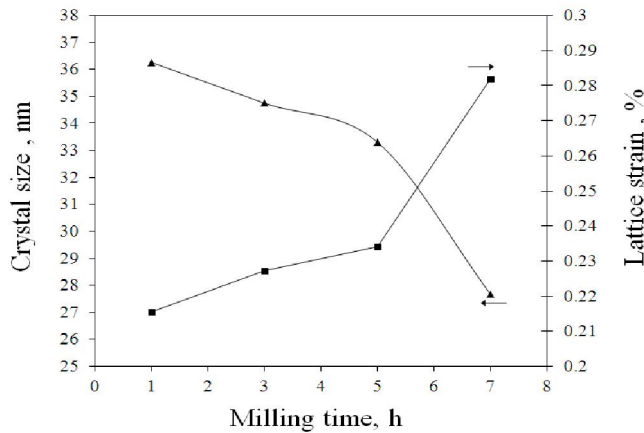Figure 5. Lattice parameter versus milling time of Al-5 wt% Al_2O_3 powder mixtures

Figure 6. Crystaliite size and lattice strain of Al-5 wt% Al_2O_3 versus milling time

3.1.2. Morphology of the prepared powders

The morphology and particle sizes are important factors in powder metallurgy. Fig. (7) shows the obtained TEM images of the powder composites milled for 1, 3, 5, and 7 h. Inspecting these images, it is evidenced that the particle size decreased with increasing milling time and no evidence of particle coarsening. During milling, the powder raw aluminum and alumina is continually intermixed leading to a homogenous material with a uniform dispersed second phase. This may be due to the used high-energy milling technique, where the collision with milling balls enhances the powder refinement. Fine and hard alumina particles are also act as milling agent, which help to reduce the powder size [23,24]. It is well known fact that the stages of milling in metal matrix powder composites include plastic deformation of the ductile matrix, fragmentation of brittle particles, micro-welding and fracturing of the deformed particles [21, 23]. In this

situation, where more fractures are formed, a large amount of fresh particle surfaces are produced with more distribution of alumina particle. This is because mechanical alloying breaks up and continually embeds the alumina particles into aluminum matrix by repeating fracturing and cold welding of the charged powders [25], and hence the particle size decreased with increasing milling time as can be shown in Fig. (8).
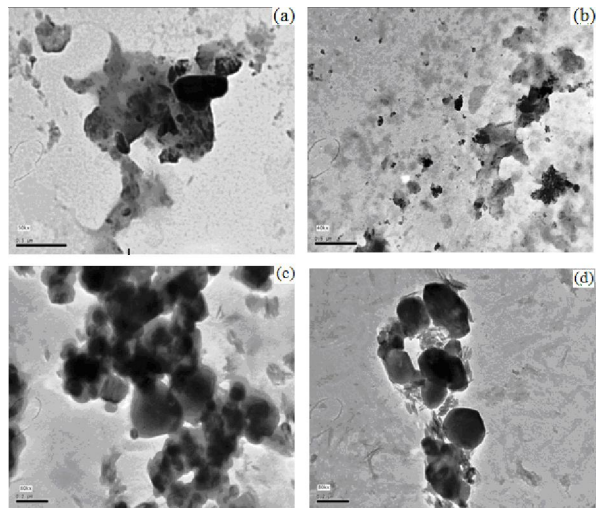

Figure 7. TEM photomicrographs of Al-5 wt% Al_2O_3 composites after different milling time, (a) 1 h, (b) 3 h, (c) 5 h, and (d) 7 h
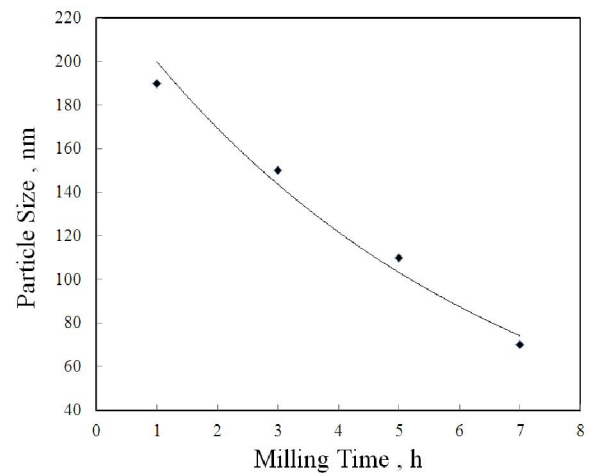

Figure 8. Particle size of Al-5 wt% Al_2O_3 composite versus milling time

3.2. Effect of sintering temperature on the sintered composites
3.2.1. Physical properties

The relative density (RD) and apparent porosity (AP) of Al- 5wt% Al_2O_3 nano-composites sintered at different temperatures (300, 370 and

470 ºC) for 1 h in argon atmosphere, are illustrated in Table (1). The RD increased with increasing both the milling time and sintering temperature, while the AP shows gradual decrease. This may be due to the refinement of particles of the milled powders [26-29].

3.2.2. Microstructure of the sintered composites

Fig. (9) exhibits the obtained optical micrographs for the Al-5 wt.% Al_2O_3 composites prepared from powder milled for 1, 3, 5 & 7 h, respectively and sintered for 1 h at 470 ºC in argon atmosphere. Inspecting these images, it can be stated generally that, as the milling time was gradually increased homogeneous microstructure is obviously observed. It is evidenced also that mechanical alloying has caused appreciable grain size reduction and consequently more grain boundaries are formed.

With increasing milling time and grain size reduction, some agglomerated particles are formed due to the formation of highly reactive particles preventing a good contact between aluminum particles during compaction [29]. It indicated also that with increasing milling time of the starting powders, the grain size of the particles decreased.

Fig. (10) shows the SEM micrograph of the Al-5 wt% Al_2O_3 composite milled for 7 h and sintered at 470ºC for 1h in argon atmosphere. This micrograph indicates that dense and homogenous microstructure with fine grains has been formed. Its Energy Dispersive Spectroscopic (EDS) analysis is also shown in Fig. (11), where only the peaks of Al (81.8%) and O (18.2%) are detected (as supplied by the apparatus software).

Table 1. Effect of milling time and sintering temperature on BD, RD and AP of Al-5 wt% Al_2O_3 composites.

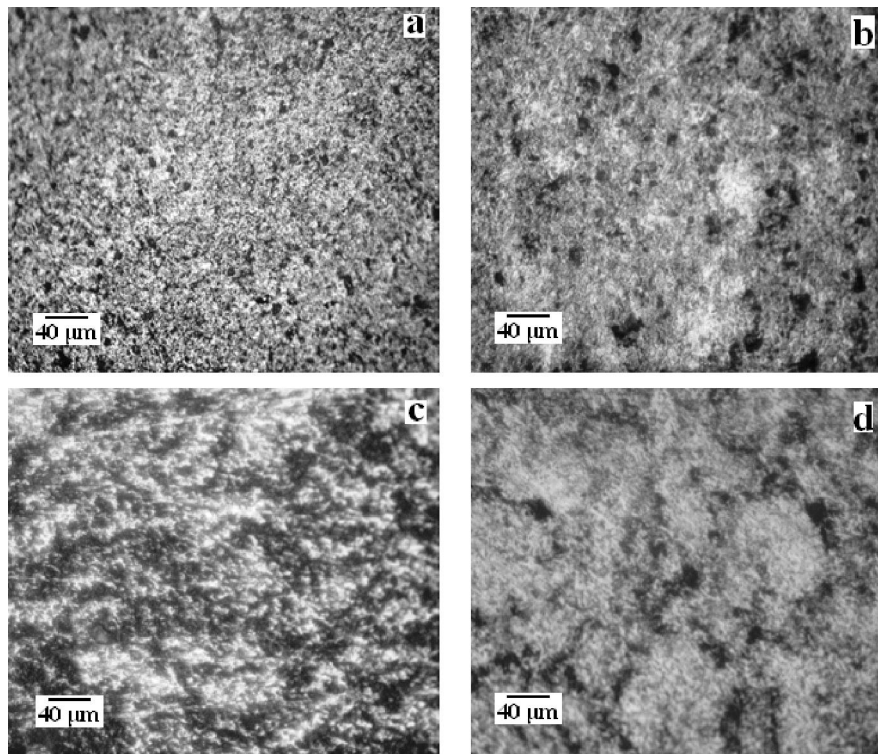| Milling Time	BD, g/cm³			TD	RD, %			AP, %		
	300ºC	370ºC	470ºC		300ºC	370ºC	470ºC	300ºC	370ºC	470ºC
1h	2.31	2.43	2.54	2.76	83.58	88.01	91.98	22.87	14.22	7.32
3h	2.34	2.46	2.60	2.76	84.69	89.28	94.30	20.11	11.75	5.04
5h	2.44	2.52	2.64	2.76	88.33	91.21	95.73	17.42	9.74	3.60
7h	2.52	2.56	2.64	2.76	91.21	92.64	95.77	16.65	7.76	2.80

Figure 9. Optical photomicrographs of Al-5 wt% Al_2O_3 milled for different times. (a) 1 h, (b) 3 h, (c) 5 h and (d) 7 h, and sintered for 1 h at 470 °C.
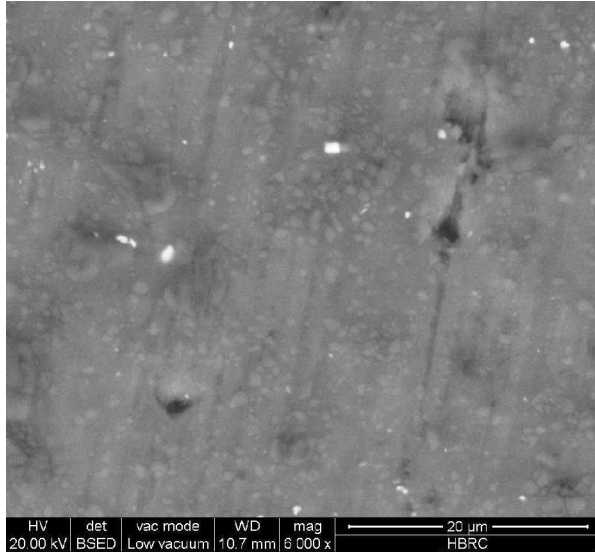
Figure 10. SEM photomicrograph of Al-5 wt% Al_2O_3 milled for 7 h and sintered at 470 °C for 1 h.
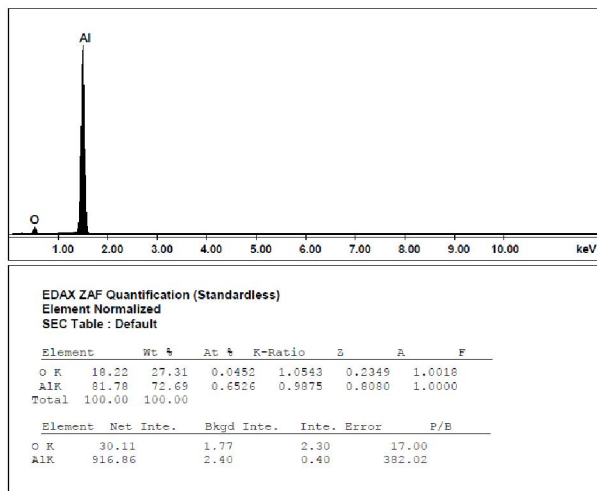

Figure 11. EDX spectrum of Al-5 wt% Al_2O_3 composite milled for 7 h and sintered for 1 h at 470 °C.

3.2.3. Micro-hardness of the sintered composites

Figure (12) shows the micro-hardness of Al-5 wt.-% Al_2O_3 composites, milled for 1, 3, 5 & 7 h, respectively and sintered for 1 h at 470ºC in argon atmosphere. It appeared that, the micro-hardness of the sintered composites increased with increasing milling time of the starting powders [20, 30, and 31]. However, it can be supposed that such increase of micro-hardness is a consequence of the dispersion of the fine Al_2O_3 particles throughout the Al metal matrix and the grain size refinement of the starting powders which led to increase the sinterability and hence, lowering the porosity. It can be supposed also

that, before milling the particle distribution was not uniform and the distance between alumina particles was so high. But starting milling and increasing its time gradually, this causes the breakage of the big and brittle alumina powders and distribute them throughout the ductile aluminum powders, and hence the distance between alumina particles decreased gradually inside the obtained metal matrix composite [32].
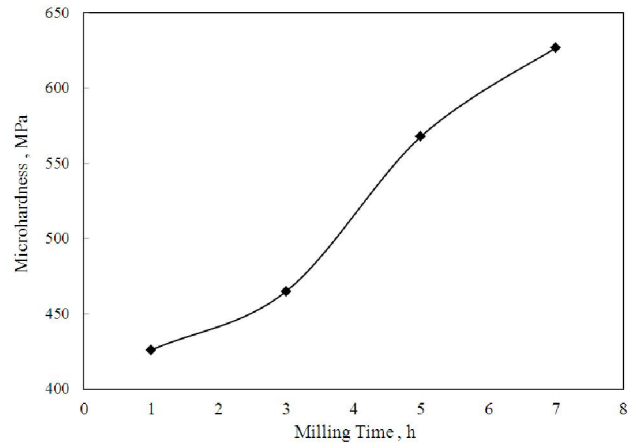

Figure 12. Micro-hardness of Al-5 wt% Al_2O_3, sintered at 470 °C versus milling time.

4. Conclusion

The obtained results can be summarized as follow:

- Mechanical alloying technique can be succesfully used to fabricate Al- 5 wt% Al_2O_3 nanocomposite after milling up to 7h.
- As the milling time was gradually increased, the crystallite size decreased and the lattice micro-strain increased, which may be due to the distortion effect caused by lattice dislocation. While the lattice parameters remain constant.
- It was confirmed that the particle size decreased gradually with increasing milling time of the Al-5 wt. % Al_2O_3 powder composite. The fine dispersion of nano-scale Al_2O_3 particles through the Al metal matrix induces changes in the structure and properties of the obtained composites.
- Increasing milling time and sintering temperature of the compressed bodies act to increase the relative density and to decrease the apparent porosity.
- Refinement of grains and dispersion of Al_2O_3 particles in the obtained metal matrix composites have considerable effect on their hardness. The nano-size Al_2O_3 particles act as strong strengthening parameter of Al matrix. However the micro-hardness of the sintered bodies was

137

found to be progressively increased with increasing milling time.

Corresponding Author:
Prof. Dr. Ahmed G. Mostafa
Faculty of Science
Physics Department
Al-Azhar University, Nasr City, Cairo, Egypt
E-mail: drahmedgamal@yahoo.com

References
1. K. R. Ahmed, S. B. J. Amaludin, L. B. Hussain, and Z. A. Ahmed, Teknologi J. (A), 42 (2005) 49.
2. V. K. Lindroos, and M. J. Talvitie, J. Materials Processing Technology, 53 (1995) 273.
3. B. Prabhu, C. Suryanarayana, L. Ana, and R. Vaidyanathan, Mater. Sci. Eng.(A), 425 (2006) 192.
4. M. F. Zawrah, H. Abdel-kader, and N. E. Elbaly, Materials Research Bulletin, 47 (2012) 655.
5. T. J. A. Doel, and P. Bowen, Composites (A), 27 (1996) 655.
6. S. S. Tousi Razavi, Rad R. Yazdani, E. Salahi, I. Mobasherpour, and M. Razavi, Powder Technology, 192 (2009) 346.
7. M. F. Zawrah, R. A. Essawy, H. A. Zayed, A. H. Abdel Fattah and M. A. Taha, Ceramics International, 40 (2014) 31.
8. C. Suryanarayana, J. Alloys and Compounds, 509 (2011) 229.
9. S. M. Zebarjad and S. A. Sajjadi, Materials and Design, 27 (2006) 684.
10. J. Naser, W. Riehemann and H. Ferkel, Mater. Sci. Eng. (A), 467 (1997) 234.
11. P. Scherrer, Gottinger Nachrichten, 2 (1918) 98.
12. S. Sivasankaran, K. Sivaprasad, R. Narayanasamy, and P. V. Satyanarayana, Materials Characterization, 62 (2011) 661.
13. S. N. Danilchenko, O. G. Kukharenko, C. Moseke, I. YU. Protsenko, L. F. Sukhodub and B. Sulkio-Cleff, Cryst. Res. Technol., 11 (2002) 1234.
14. H. P. Klug, "X-Ray Diffraction Procedures for Crystalline and Amorphous materials", E. Alexander, 2nd edition. John Wiley and Sons, New York (1974).
15. K. M. Youssef, R. O. Scattergood, K. L. Murty and C. C. Koch, Scripta Materialia, 54 (2006) 251.
16. R. S. Liu, W. C. Shi, Y. C. Cheng and C. Y. Huang, Mod. Phys. Lett. (B), 11 (1997) 1169.
17. M. M. Moustafa, A. Elkady Omayma, and Abdelhameed Wazeer Abdelhameed, Open J. of Metal, 3 (2013) 72.
18. M. S. Aboraia, G. A. Abdalla, and H. S. Wasly, Int. J. of Engineering Research and Applications, 3 (2013) 1654.
19. C. Suryanarayana, Mechanical alloying Prog. Mater. Sci., 46 (2001) 184.
20. D. Bozic, J. Stasic, B. Dimcic, M. Vilotijevic and V. Bull. Rajkovic, Mater. Sci., 34 (2011) 217.
21. Mostafa Alizadeh and Morteza Mirzaei Aliabadi, J. Alloys and Compounds, 509 (2011) 4978.
22. Z. Hesabi Razavi , A. Simchi and S. M. Seyed Reihani, Mater. Sci. Eng. (A), 428 (2006) 159.
23. J. B. Fogognolo, F. Velasco, M. H. Robert and J. M. Torralba, Mater. Sci. Eng. (A), 342 (2003) 131.
24. S. S. Razavi Tousi, R. Yazdani Rad, E. Salahi, M. R. Rahimipour, A. Kazemzade and M. Razavi, J. Materials and Energy Research Center, 22 no. 2 (2009) 177.
25. Zuhailawati Hussain, and Leong Chee Kit, Materials and Design, 29 (2008) 1311.
26. M. F. Zawrah, R. A. Essawy, H. A. Zayed, A. H. Abdel Fattah, M. A. Taha, Materials and Design, 46 (2013) 485.
27. Korac Marija, Andic Zoran, Tasic Miloš and Kamberovic Z̆eljko, J. Serb. Chem. Soc., 72, (11) (2007) 1115.
28. G. S. Hanumanth, and G. A. Irons, J. Mater. Sci., 28 (1993) 2459.
29. P. K. Ghost and S. Ray, AFS Trans., (1988) 775.
30. F. Shehata, A. Fathy, M. Abdelhameed and S. F. Moustafa, Materials and Design, 30 (2009) 2756.
31. J. L. Hernández Rivera, J. J. Cruz Rivera, V. Paz del Ángel, Garibay Febles, V. O. Coreño Alonso and R. Martínez-Sánchez, Materials and Design, 37 (2012) 96.
32. S. M. Zebarjad, and S. A. Sajjadi, Materials and Design, 27 (2006) 684.

2/26/2015